Int. J. Solids Structures Vol. 28, No. 4, pp. 449–469, 1991
Printed in Great Britain.

0020–7683/91 $3.00 + .00

RESIDUAL STRESSES IN SYMMETRIC, DOUBLE LAP AND DOUBLE STRAP JOINTS

MING-HWA R. JEN, WEN-SEN LIN and JER-MING HSU
Department of Mechanical Engineering, National Sun Yat-Sen University, Kaohsiung, Taiwan 80424, R.O.C.

(*Received* 23 *February* 1990; *in revised form* 28 *November* 1990)

Abstract—This work presents a one-dimensional analysis of the bonding stresses at the interfaces between the adhesive bond lines and the adherents for both the symmetric, double lap and double strap joints, due to several typical moisture profiles distributed along the adhesive material. The analysis considers linear elastic behavior and presupposes the forms of kinematic fields. The formulation then follows variational principles and the interlaminar stresses are evaluated as Lagrange multipliers which are incorporated into the internal energy. Based on the derivation of linear elastic residual stresses, linear viscoelastic solutions are also obtained by Direct Method. The finite element method (FEM) is adopted to yield numerical predictions in comparison with the linear elastic and viscoelastic solutions. The stresses along the normalized length, the x-axis, are very close for $0 \leqslant x \leqslant 0.7$; for $0.7 < x \leqslant 1$ both linear elastic and viscoelastic solutions are very close and the FEM solution reaches singularity at the free edge due to the so-called edge effect. In addition, the theoretical and numerical results all indicate that the most detrimental stresses arise at the free edges during moisture desorption.

NOMENCLATURE

As	non-dimensional terms
Bs	non-dimensional terms
Cs	non-dimensional terms
a	thickness of adhesive
c	length of outer adherent
D	compliance
E	Young's modulus
e	adhesive layer
F	body force density
fs	non-dimensional terms
g	power of time
h	thickness of adherent
i	sub index
j	sub index
Ks	constants
ks	non-dimensional terms
L	left
M	moment of resultant
m	moisture distribution
N	normal stress resultant
P	non-dimensional interlaminar normal stress
p_1, p_2	interlaminar normal stress
q_1, q_2	interlaminar shear stress
Q	shear resultant
Rs	non-dimensional terms
r	right side
S	transverse stress resultant
s	Laplace transform factor
T	traction
$T_{1,2}$	non-dimensional interlaminar tangential stresses
t	time
U	internal energy
W	external work
u	displacement in x-axis
v	displacement in y-axis
w	displacement in z-axis
x	axis
y	axis
z	axis
1	central adherent
1*e*	adhesive filler

2	outer adherent
β	moisture expansion coefficient
δ	variation
ε	strain
Λ	Lamé constant
μ	Lamé constant
ν	Poisson's ratio
φ	non-dimensional term
η	non-dimensional term
σ	normal stress
τ	shear stress
*	external traction

INTRODUCTION

Adhesively bonding joints have increasingly been utilized in engineering applications (Schwartz and Goodman, 1982; Schwartz, 1984) instead of mechanical joints, such as bolt, weld, rivet, etc. However, many observations have indicated that these joints may fail under long-term exposure to humidity and to various temperature changes (Hoskin and Baker, 1986).

This paper presents an analysis of the stresses which arise at the interfaces between the adhesive and the adherents of the symmetric, double lap and strap joints due to the typical moisture distributions caused by long-term environmental effects along the very thin layer of adhesive. Since the adherents are much stiffer than the adhesive, they constrain its tendency to swell and deform under moisture sorption, thereby introducing residual stresses into the joint. The analysis accounts for the bending of the outer adherents due to the expansion of the adhesive and for the compression of the inner adherents.

The problem can also be extended to the temperature effect by replacing the moisture sorption and considering the different thermal expansion coefficients for adherents and adhesive. In the case of both temperature and moisture changes, the interaction of moisture by temperature change and vice versa in adherents and adhesive will be a topic for further study. The mathematical modeling of the mechanical behavior of the joint employs variational methods and is approximate in nature. First, the response is assumed to be linear elastic. Then, the response can actually be better described to be linear viscoelastic. Computations are performed with material properties that are representative of aluminum adherents and epoxy adhesive in linear elastic, linear viscoelastic and finite element methods.

To date there exist some investigations which consider the effects of non-uniform, time-transient moisture and/or temperature distributions on the mechanical response of materials and structures (Crossman *et al.*, 1979; Flaggs and Crossman, 1979; Ramanko and Kanus, 1980; Weitsman, 1977a,b, 1979, 1980; Jen and Weitsman, 1981). Some of these papers (Crossman *et al.*, 1979; Weitsman, 1977b) deal with moisture affected material response while others (Flaggs and Crossman, 1979; Ramanko and Kanus, 1980; Weitsman, 1977a, 1979, 1980; Jen and Weitsman, 1981) evaluate moisture-induced stresses in adhesive joints. Of the latter, Flaggs and Crossman (1979) and Ramanko and Kanus (1980) provide numerical solutions.

In view of the high degree of complexity involved in describing the multi-faceted effects of moisture, especially on the response of the adhesive, it is obvious that any detailed accounting must be done by means of numerical methods. However, this very same complexity justifies an independent evaluation based upon idealized assumptions whose aim is to provide at least partial verification of the numerical results. The present work strives to fulfil this task.

LINEAR ELASTIC FORMULATION

Consider the symmetric, double lap joint shown in Fig. 1a and the double strap joint in Fig. 1b. There is, however, an ambiguity in the definition of the symmetric, double lap joint (Fig. 1a), some researchers calling Fig. 1a a double lap joint without a central adherent and some calling Fig. 1b a double doubler joint. Due to the geometric symmetry it is

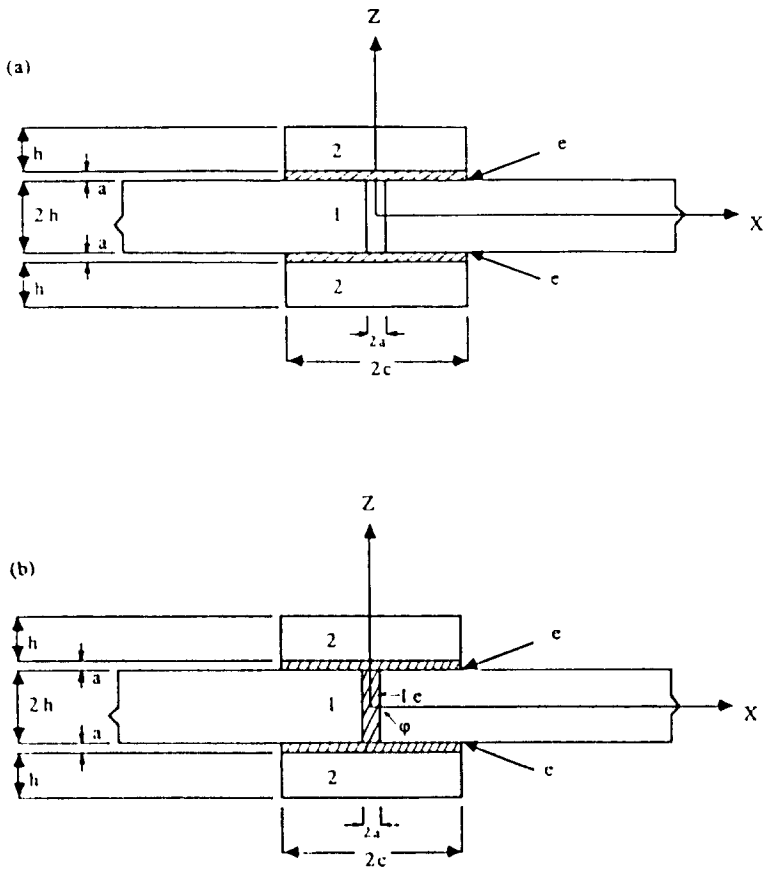

Fig. 1. The geometry of the symmetric, double lap and double strap joints. (a) Symmetric, double lap joint. (b) Double strap joint.

sufficient to analyze only the first quadrant, $x \geqslant 0$, $z \geqslant 0$. The moisture profiles are also assumed to be symmetric in both x and z axes. The induced swelling strains into the adhesive layer which, constrained by more rigid adherents "1" and "2", gives rise to internal stresses in the joint. We also aim to analyze the displacements of "2".

A. *Stress–strain relations*

First we consider linear elastic response, assuming plane strain ($\varepsilon_y = 0$), and regard the outer adherents to deform as plates by employing Kirchhoff's relation (Donnell, 1976) in the bending theory of isotropic plates, since it is purely kinematic in form. Let $m = m(x)$ denote the moisture distribution induced by moisture sorption; then, denoting the Lamé constants by Λ and μ we have the following stress-strain relations.

(a) *In* "1" (*central adherent*).

$$\sigma_x = (\Lambda + 2\mu)\varepsilon_x + \Lambda\varepsilon_z, \quad \sigma_z = (\Lambda + 2\mu)\varepsilon_z + \Lambda\varepsilon_x. \tag{1}$$

Denoting the displacements by u_1 and w_1, and discarding the shear, we assume the strain-displacement relations for this adherent:

$$\varepsilon_x = u', \quad \varepsilon_z = \frac{w_1}{h}. \tag{2}$$

In eqn (2) and in the following primes denote derivatives with respect to x.

(b) *In* "2" (*outer adherent*). Following the beam theory approximation we consider $\varepsilon_y = 0$ and $\sigma_z = 0$; then, by Hooke's Law, we obtain

$$\varepsilon_x = \frac{1-\nu^2}{E}\sigma_x. \tag{3}$$

Denoting the displacements in this adherent by u_2 and w_2, and following classical beam theory, we obtain

$$\varepsilon_x = u_2' - zw_2''. \tag{4}$$

(c) *In* "e" (*adhesive layer*).

$$\begin{aligned}\sigma_x &= (\Lambda_e + 2\mu_e)\varepsilon_x + \Lambda_e\varepsilon_z - (3\Lambda_e + 2\mu_e)\beta m\\ \sigma_z &= \Lambda_e\varepsilon_x + (\Lambda_e + 2\mu_e)\varepsilon_z - (3\Lambda_e + 2\mu_e)\beta m\\ \tau_{xz} &= \mu_e\gamma_{xz}.\end{aligned} \tag{5}$$

In eqn (5) $m = m(x)$ is the moisture content and β denotes the moisture expansion coefficient.

In view of its exceedingly small thickness we now assume the displacement u to vary linearly in z, namely, $u = u_e + z\gamma_e$. In addition, denoting by w^+ and w^- the vertical displacements at the top and bottom of the adhesive layer we assume $\varepsilon_z = (w^+ - w^-)/a$. Then, we consider the shear strain $\gamma_{xz} = \tau_{xz}/G_e = (u^+ - u^-)/a = \gamma_e$. Finally, $\varepsilon_x = u_e' + z\gamma_e'$, $u^- = u_e - a\gamma_e/2$, $u^+ = u_e + a\gamma_e/2$.

(d) *In* "1e" (*adhesive filler*). For the double strap joint, the equations are the same as eqn (1), except for adding subscript e in Lamé constants and strains. We also assume the displacement u to vary linearly in z for the adhesive layer.

B. *Stress resultants*

In order to evaluate the internal and external work, we now define some stress resultants with respect to each center line in the local coordinates as follows.

(a) *In* "1" (*central adherent*).

$$N_1 = \int_0^h \sigma_x\,dz = (\Lambda + 2\mu)hu_1' + \Lambda w_1, \quad S_1 = \int_0^h \sigma_z\,dz = \Lambda hu_1' + (\Lambda + 2\mu)w_1. \tag{6}$$

(b) *In* "2" (*outer adherents*).

$$N_2 = \int_{-h/2}^{h/2} \sigma_x\,dz = \frac{Eh}{1-\nu^2}u_2', \quad M_2 = \int_{-h/2}^{h/2} z\sigma_x\,dz = -\frac{E}{1-\nu^2}\frac{h^3}{12}w_2''. \tag{7}$$

(c) *In* "e" (*adhesive layer*).

$$\begin{aligned}N_e &= \int_{-a/2}^{a/2} \sigma_x\,dz = (\Lambda_e + 2\mu_e)au_e' + \Lambda_e(w_2 - w_1) - (3\Lambda_e + 2\mu_e)a\beta m\\ S_e &= \int_{-a/2}^{a/2} \sigma_z\,dz = \Lambda_e au_e' + (\Lambda_e + 2\mu_e)(w_2 - w_1) - (3\Lambda_e + 2\mu_e)a\beta m\\ Q_e &= \int_{-a/2}^{a/2} \tau_{xz}\,dz = \mu_e a\gamma_e\\ M_e &= \int_{-a/2}^{a/2} z\sigma_x\,dz = \frac{a^3}{12}(\Lambda_e + 2\mu_e)\gamma_e'.\end{aligned} \tag{8}$$

In the first two parts of eqn (8) we employed the continuity conditions $w^+ = w_2$, $w^- = w_1$.

(d) *In "1e" (adhesive filler).*

$$N_{1e} = \int_0^h \sigma_x \, dz = (\Lambda_e + 2\mu_e)hu'_{1e} + \Lambda_e w_{1e} - (3\Lambda_e + 2\mu_e)h\beta m$$

$$S_{1e} = \int_0^h \sigma_z \, dz = \Lambda_e hu'_{1e} + (\Lambda_e + 2\mu_e)w_{1e} - (3\Lambda_e + 2\mu_e)h\beta m. \tag{9}$$

Equations (6)–(9) are the stress resultants obtained by the substitution of stresses of eqns (1)–(5).

C. *Principle of virtual work and governing equations*

We now employ the principle of virtual work $\delta U = \delta W$, where δU and δW are the variations of internal and external work, respectively, as formulated in terms of kinematically admissible displacement fields (Dym and Shames, 1973). In our formulation we shall ascertain the continuity of all displacements, at the interfaces between adhesive and adherents, by employing Lagrange multipliers q_1, q_2, p_1 and p_2, respectively. We thus have

$$\begin{aligned}\delta U = \int_0^c & N_2\delta u'_2 - M_2\delta w''_2 + N_e\delta u'_e + \frac{1}{a}S_e(\delta w^+ - \delta w^-) + M_e\delta\gamma'_e \\ & + Q_e\delta\gamma_e + N_1\delta u'_1 + \frac{1}{h}S_1\delta w_1 + q_2\left(\delta u_2 + \frac{h}{2}\delta w'_2 - \delta u_e - \frac{a}{2}\delta\gamma_e\right) \\ & + q_1\left(\delta u_e - \delta u_1 - \frac{a}{2}\delta\gamma_e\right) + p_2(\delta w_2 - \delta w^+) + p_1(\delta w^- - \delta w_1) \\ & + \delta q_2\left(u_2 + \frac{h}{2}w'_2 - u_e - \frac{a}{2}\gamma_e\right) + \delta q_1\left(u_e - u_1 - \frac{a}{2}\gamma_e\right) \\ & + \delta p_2(w_2 - w^+) + \delta p_1(w^- - w_1)\,dx.\end{aligned} \tag{10}$$

Integration-by-parts of eqn (10) and collection of terms which multiply each of the independent variations δu_1, δu_2, δu_e, δw_1, δw_2, δw^+, δw^-, δq_1, δq_2, δp_1, δp_2 and $\delta\gamma_e$ yield the following field equations:

$$\begin{aligned} -N'_1 - q_1 &= 0 \\ -N'_2 + q_2 &= 0 \\ -N'_e - q_2 + q_1 &= 0 \\ Q_e - \frac{a}{2}q_2 - \frac{a}{2}q_1 - M'_e &= 0 \\ \frac{1}{h}S_1 - p_1 &= 0 \\ -M''_2 - \frac{h}{2}q'_2 + p_2 &= 0 \\ \frac{1}{a}S_e - p_2 &= 0 \\ -\frac{1}{a}S_e + p_1 &= 0 \end{aligned}$$

$$u_2+\frac{h}{2}w_2'-u_e-\frac{a}{2}\gamma_e=0$$

$$u_e-\frac{a}{2}\gamma_e-u_1=0$$

$$w_2-w^+=0$$

$$w^--w_1=0. \tag{11a-l}$$

Equation 11(i-l) expresses the continuity conditions of displacements at the interfaces, which verifies that our previous assumptions are correct.

Denoting components of external traction with an asterisk, we have the following expression commensurate with the integration-by-parts of eqn (10):

$$\delta W=\left[N_e^*\delta u_e+M_e^*\delta\gamma_e+N_1^*\delta u_1+N_2^*\delta u_2+\left(M_2^{*\prime}+\frac{h}{2}q_2^*\right)\delta w_2-M_2^*\delta w_2'\right]_0^c.$$

Note that the Lagrange multipliers p_1, p_2, q_1 and q_2, which are the force conjugates of the vertical and horizontal displacements at the interfaces, represent the interlaminar normal and shear stresses. Equation (11) gives

$$q_1=\tfrac{1}{2}N_e'+\frac{1}{a}Q_e-\frac{1}{a}M_e', \quad q_2=-\tfrac{1}{2}N_e'+\frac{1}{a}Q_e-\frac{1}{a}M_e',$$

$$p_1=p_2=\frac{1}{a}S_e=M_2''+\frac{h}{2}q_2'. \tag{12}$$

Proceeding in the standard manner, and eliminating u_1 and u_2 with the aid of eqn (11i,j), we obtain the "natural" boundary conditions for our problem from the components in the variational form of external traction, δW, and conclude that following kinematic or traction quantities must be prescribed at $x=0$ and $x=c$:

$$u_e \quad \text{or} \quad N_1+N_2+N_e \quad \text{and}$$

$$\gamma_e \quad \text{or} \quad \frac{a}{2}N_2-\frac{a}{2}N_1+M_e \quad \text{and}$$

$$w_2 \quad \text{or} \quad M_2'+\frac{h}{2}q_2 \quad \text{and}$$

$$w_2' \quad \text{or} \quad -\frac{h}{2}N_2-M_2. \tag{13a-d}$$

At this point we note that eqn (11a-c) yields $N_1+N_2+N_e=\text{constant}$. In the absence of external loads we get $N_1+N_2+N_e=0$, whereby this field relation automatically incorporates the traction-free boundary condition listed in eqn (13a). For instance, the right part of eqn (13b) is produced by substituting eqn (11a) and eqn (11b) into eqn (11d) and then integrating.

Omitting eqn (13a), which must be satisfied as a field equation, we get at the traction-free boundary $x=c$:

$$\frac{a}{2}(N_2-N_1)+M_e=0 \tag{14}$$

$$M_2'+\frac{h}{2}q_2=0$$

$$-\frac{h}{2}N_2-M_2=0.$$

Symmetry considerations provide us with the following four boundary conditions at $x = 0$:

$$u_e = 0$$
$$\gamma_e = 0$$
$$w_2' = 0$$
$$M_2' + \frac{h}{2} q_2 = 0. \tag{15}$$

We now introduce the non-dimensional moduli ratios

$$\frac{\Lambda_e + 2\mu_e}{3\Lambda_e + 2\mu_e} = f_1, \quad \frac{\Lambda_e}{3\Lambda_e + 2\mu_e} = f_2, \tag{16a}$$
$$\frac{\mu_e}{3\Lambda_e + 2\mu_e} = f_3, \quad \frac{\Lambda + 2\mu}{3\Lambda_e + 2\mu_e} = f_4,$$
$$\frac{\Lambda}{3\Lambda_e + 2\mu_e} = f_5, \quad \frac{E/1 - \nu^2}{3\Lambda_e + 2\mu_e} = f_E,$$

the non-dimensional distances and variables

$$\frac{h}{c} = \eta, \quad \frac{a}{c} = \varphi, \quad x^{ND} = \frac{x}{c}, \tag{16b}$$

and the non-dimensional kinematic variables

$$w_1 = a w_1^{ND}, \quad w_2 = a w_2^{ND}, \quad u_e = a u_e^{ND}, \quad \gamma_e = \gamma_e^{ND}. \tag{16c}$$

Elimination of p_1, p_2, q_1, q_2, u_1, u_2, w^+ and w^- from eqn (11), employment of eqn (8), non-dimensionalization of eqn (16) and after several manipultions of eqn (11c–f) yields

$$A_1 D u_e + A_2 D\gamma_e + A_3 w_1 + (A_4 D^2 + A_5) w_2 = \beta m$$
$$-\varphi A_2 D^2 u_e + (A_6 D^2 + A_7)\gamma_e + A_8 D w_1 - \frac{\varphi A_4}{2} D^3 w_2 = 0$$
$$\varphi A_3 D u_e - A_8 D\gamma_e + A_9 w_1 + A_{10} w_2 = -\beta m$$
$$(\varphi A_4 D^3 + \varphi A_5 D) u_e + \frac{\varphi A_4}{2} D^3 \gamma_e + A_{10} w_1 - \left(\frac{2\eta\varphi A_4}{3} D^4 + A_{10}\right) w_2 = \beta m. \tag{17a–d}$$

In eqn (17) D designates derivative with respect to x^{ND} and all variables are non-dimensional. The expressions for A_i are given in eqns (A1) in the Appendix.

In a similar manner we can obtain the non-dimensional version of the seven boundary conditions, eqns (14) and (15), at $x^{ND} = 0$ and $x^{ND} = 1$, and expressions for the non-dimensional interlaminar stresses q_1, q_2, p_1 and p_2.

The system eqn (17) is of seventh order in the operator D, commensurate with the seven boundary conditions, eqns (14) and (15). To solve our boundary value problem we wish to represent eqn (17) by a system of first order differential equations. This reduction cannot be accomplished directly because a straightforward procedure, e.g., $Du_e = X_1$, $D^2 u_e = X_2$, $D^3 u_e = X_2'$, etc., would introduce extraneous redundancies. To avoid these redundancies we first eliminate w_1 from eqn (17c) and then differentiate and combine the remaining equations to lower the order of the highest derivative of u_e (Jen, 1980). In this

manner we obtain the equivalent system:

$$\begin{aligned} B_1 Du_e + B_2 D\gamma_e + (B_3 D^2 + B_4) w_2 &= C_1 \beta m \\ (B_5 D^2 + B_7)\gamma_e + (B_{18} D^3 + B_{19} D) w_2 &= C_5 \beta m' \\ B_{11} Du_e + B_{14} D\gamma_e + (B_{15} D^4 + B_{16} D^2 + B_{13}) w_2 &= C_4 \beta m'' + C_3 \beta m. \end{aligned} \tag{18}$$

The expressions for B_i and C_i are given in eqns (A2) in the Appendix. We now denote

$$\begin{aligned} &X_1 = u_e, \quad X_1' = Du_e, \quad X_2 = \gamma_e, \quad X_3 = X_2', \\ &X_4 = w_2, \quad X_5 = X_4', \quad X_6 = X_5', \quad X_7 = X_6'. \end{aligned} \tag{19}$$

The system (18) then reads

$$\begin{bmatrix} B_1 & 0 & 0 & 0 & 0 & 0 & 0 \\ 0 & 1 & 0 & 0 & 0 & 0 & 0 \\ 0 & 0 & B_{17} & 0 & 0 & 0 & 0 \\ 0 & 0 & 0 & 1 & 0 & 0 & 0 \\ 0 & 0 & 0 & 0 & 1 & 0 & 0 \\ 0 & 0 & 0 & 0 & 0 & 1 & 0 \\ B_{11} & 0 & 0 & 0 & 0 & 0 & B_{15} \end{bmatrix} \cdot \begin{bmatrix} X_1 \\ X_2 \\ X_3 \\ X_4 \\ X_5 \\ X_6 \\ X_7 \end{bmatrix} =$$

$$\begin{bmatrix} 0 & 0 & -B_2 & -B_4 & 0 & -B_3 & 0 \\ 0 & 0 & 1 & 0 & 0 & 0 & 0 \\ 0 & -B_7 & 0 & 0 & -B_{19} & 0 & -B_{18} \\ 0 & 0 & 0 & 0 & 1 & 0 & 0 \\ 0 & 0 & 0 & 0 & 0 & 1 & 0 \\ 0 & 0 & 0 & 0 & 0 & 0 & 1 \\ 0 & 0 & -B_{14} & -B_{13} & 0 & -B_{16} & 0 \end{bmatrix} \begin{bmatrix} X_1 \\ X_2 \\ X_3 \\ X_4 \\ X_5 \\ X_6 \\ X_7 \end{bmatrix} + \begin{bmatrix} C_1 \beta m \\ 0 \\ C_5 \beta m' \\ 0 \\ 0 \\ 0 \\ C_4 \beta m'' + C_3 \beta m \end{bmatrix}. \tag{20}$$

Written compactly, eqn (20) reads

$$[A](X') = [B](X) + (C)$$

whereby

$$(X') = [D](X) + (E)$$

with

$$[D] = [A]^{-1}[B], \quad (E) = [A]^{-1}(C). \tag{21}$$

D. *Solution of equations*

The solution scheme deviates from the standard method (Hochstadt, 1963; Kolman, 1965; Coddington and Levinson, 1955), because ours is a boundary value, not an initial value problem.

The complete solution (**X**) is formed by superposition of a particular solution ($\mathbf{X}_p$) and a complementary solution (**W**). The particular solution ($\mathbf{X}_p$) is taken to satisfy eqn (21) with null initial conditions ($\mathbf{X}_p(0)$) = (**0**) and can be formed by standard methods. The complementary solution (**W**) is constructed by considering (**E**) = (**0**) in eqn (21) and in a

manner which, together with $(\mathbf{X}_p)$, satisfies the boundary conditions at $x = 0$ and $x = 1$. Note that $(\mathbf{X})$, $(\mathbf{X}_p)$ and $(\mathbf{W})$ are seven-dimensional vectors.

Employing eqn (19), the non-dimensional boundary conditions are:

$$\begin{aligned} X_1(0) = 0, \quad X_2(0) = 0, \quad X_5(0) = 0, \\ 4\eta X_7(0) - 3X_3'(0) - 6X''_1(0) = 0, \\ 4\eta X_6(1) - 3X_3(1) - 6X'_1(1) = 0, \\ 4\eta X_7(1) - 3X_3'(1) - 6X''_1(1) = 0, \\ R_1 X'_1(1) + R_2 X_3(1) + R_3 X_6(1) + R_4 X_4(1) = R_5 \beta m(1). \end{aligned} \tag{22}$$

The expressions for R_i are given in eqns (A3) in the Appendix.

Since much of what follows accords with standard methods (Hochstadt, 1963; Kolman, 1965; Coddington and Levinson, 1955), we shall omit details to retain brevity; a complete analysis is given in Jen (1980).

To determine the particular solution we consider the eigenvalue problem $[D]^T + \lambda[I] = 0$ which yields seven eigenvalues, one of which, say λ_1, turns out to be $\lambda_1 = 0$, with the remaining six values generally being complex. Denoting the distinct eigenvalues by $\lambda_1, \lambda_2, \ldots, \lambda_7$, and the corresponding eigenvectors by $(a_1), (a_2), \ldots, (a_7)$, it can be shown that

$$(a_{1j}) = (1, a_{12}, 0, 0, a_{15}, 0, a_{17})^T \quad \text{and} \quad (a_{ij}) = (0, 1, a_{i3}, a_{i4}, a_{i5}, a_{i6}, a_{i7})^T, \quad i = 2, 3, \ldots, 7$$

with components expressed in terms of $B_1, B_2, \ldots, B_{10}$, derived before by Jen (1980).

We now construct the 7×7 matrix $[\phi]$ with elements $\phi_{ij} = a_{ij}^T \exp(\lambda_i x)$ (no sum on j). This matrix can be written as

$$[\phi_{ij}] = [\text{diag } e^{\lambda_i x}][a_{ij}^T]. \tag{23}$$

Consequently

$$[\phi_{ij}^{-1}] = [a_{ij}^{T\,-1}][\text{diag } e^{-\lambda_i x}] \tag{24}$$

in eqns (23) and (24); $i, j = 1, 2, \ldots, 7$.

We also form the vector $G_i(x)$ by generating

$$(H(y)) = [\phi(y)](E(y)), \quad \text{then} \quad G_i(x) = \int_0^x H_i(y)\,dy. \tag{25}$$

After several manipulations it can be shown that

$$G_1(x) = (g_1 + a_{17}g_8)\beta \int_0^x m(y)\,dy + a_{17}g_7\beta[m'(x) - m'(0)]$$

$$\begin{aligned} G_i(x) = a_{i7}g_8 \int_0^x e^{\lambda_i y} m(y)\,dy + a_{i3}g_3\beta\left[e^{\lambda_i x} m(x) - m(0) - \lambda_i \int_0^x e^{\lambda_i y} m(y)\,dy\right] \\ + a_{i7}g_7\beta[e^{\lambda_i x} m'(x) - m'(0) - \lambda_i e^{\lambda_i x} m(x) + \lambda_i m(0) + \lambda_i^2 \int_0^x e^{\lambda_i y} m(y)\,dy] \end{aligned} \tag{26}$$

(no sum on i, $i = 2, 3, \ldots, 7$.)

The particular solution (X_p) is given by

$$X_{pi} = \sum_{j=1}^{7} \phi_{ij}^{-1}(x) G_j(x) \quad i = 1, 2, \ldots, 7. \tag{27}$$

Or, in more detail

$$X_{pi} = \phi_{i1}^{-1}(x)\beta\left\{(g_1 + a_{17}g_8)\int_0^x m(y)\,dy + a_{17}g_7[m'(x) - m'(0)]\right\}$$
$$+ \sum_{k=2}^{7} \phi_{ik}^{-1}(x)\beta\left\{a_{k7}g_8\int_0^x e^{\lambda_k y} m(y) + a_{k3}g_3\left[e^{\lambda_k x} m(x)\right.\right.$$
$$- m(0) - \lambda_k\int_x^x e^{\lambda_k y} m(y)\,dy\Big] + a_{k7}g_7\Big[e^{\lambda_k x} m'(x) - m'(0)$$
$$\left.\left. - \lambda_k e^{\lambda_k x} m(x) + \lambda_k m(0) + \lambda_k^2\int_0^x e^{\lambda_k y} m(y)\,dy\Big]\right\} \quad \text{(no sum on } k\text{)}. \tag{27a}$$

As already mentioned, the construction eqn (27) satisfies $(\mathbf{X}_p(0)) = (\mathbf{0})$, but does not meet boundary conditions eqn (22).

To satisfy eqn (22) we incorporate the complementary solution (**W**). To construct (**W**) we consider $(\mathbf{W}') = [D](\mathbf{W})$, with $[D]$ given in eqn (21), and solve the characteristic equation $\det(D - \zeta I) = 0$. The components of D_{ij} are expressible in terms of $B_1, B_2, \ldots, B_{19}$ (Jen, 1980) and we again obtain seven eigenvalues ζ_i, with associated eigenvectors. As in the case of the particular solution we have a null eigenvalue, say $\zeta_1 = 0$ (Jen, 1980).

After several straightforward manipulations we get

$$W_1 = K_1 + \sum_{i=2}^{7} K_i\left\{\frac{1}{\zeta_i}\left[\frac{k_{13}}{k_{73}}(-k_{74} - k_{76}\zeta_i^2 + \zeta_i^4) + k_{14} + k_{16}\zeta_i^2\right]\right\} e^{\zeta_i x}$$

$$W_2 = \sum_{i=2}^{7} K_i\left[\frac{1}{\zeta_i}\frac{1}{k_{73}}(-k_{74} - k_{76}\zeta_i^2 + \zeta_i^4)\right] e^{\zeta_i x}$$

$$W_3 = \sum_{i=2}^{7} K_i\left[\frac{1}{k_{73}}(-k_{74} - k_{76}\zeta_i^2 + \zeta_i^4)\right] e^{\zeta_i x}$$

$$W_4 = \sum_{i=2}^{7} K_i e^{\zeta_i x}$$

$$W_5 = \sum_{i=2}^{7} K_i\zeta_i e^{\zeta_i x}$$

$$W_6 = \sum_{i=2}^{7} K_i\zeta_i^2 e^{\zeta_i x}$$

$$W_7 = \sum_{i=2}^{7} K_i\zeta_i^3 e^{\zeta_i x}. \tag{28}$$

In eqn (28) K_i, $i = 1, 2, \ldots, 7$, are arbitrary constants. The various k_{ij} are listed in eqns (A4) in the Appendix.

In view of eqns (22) and (27) we obtain the following seven equations to determine the constants K_i, $i = 1, 2, \ldots, 7$:

$$W_1(0) = 0$$
$$W_2(0) = 0$$
$$W_3(0) = 0$$
$$4\eta W_7(0) - 3W_3'(0) - 6W_1''(0) = 3\sum_{i=1}^{7}[\phi_{3i}^{-1}(0)G_i'(0) + \phi'_{3i}^{-1}(0)G_i(0)]$$
$$+ 6\sum_{i=1}^{7}[\phi_{1i}^{-1}(0)G_i''(0) + 2\phi'_{1i}^{-1}(0)G_i'(0) + \phi''_{1i}^{-1}(0)G_i(0)]$$

$$4\eta W_2(1)-3W_3(1)-6W_1''(1)=-4\eta\sum_{j=1}^{7}\phi_{2j}^{-1}(1)G_j(1)+3\sum_{j=1}^{7}[\phi_{3j}^{-1}(1)G_j'(1)$$
$$+\phi'^{-1}_{3j}(1)G_j(1)]+6\sum_{j=1}^{7}[\phi_{1j}^{-1}(1)G_j''(1)+2\phi'^{-1}_{1j}(1)G_j'(1)+\phi''^{-1}_{1j}(1)G_j(1)]$$

$$4\eta W_6(1)-3W_3(1)-6W_1'(1)=-4\eta\sum_{j=1}^{7}\phi_{6j}^{-1}(1)G_j(1)+3\sum_{j=1}^{7}\phi_{3j}^{-1}(1)G_j(1)$$
$$+6\sum_{j=1}^{7}[\phi_{1j}^{-1}(1)G_j'(1)+\phi'^{-1}_{1j}(1)G_j(1)]$$

$$R_1W_1'(1)+R_2W_3(1)+R_3W_6(1)+R_4W_4(1)=R_5\beta m(1)-R_1\sum_{j=1}^{7}[\phi_{1j}^{-1}(1)G_j'(1)$$
$$+\phi'^{-1}_{1j}(1)G_j(1)]-R_2\sum_{j=1}^{7}\phi_{3j}^{-1}(1)G_j(1)-R_3\sum_{j=1}^{7}\phi_{6j}^{-1}(1)G_j(1)$$
$$-R_4\sum_{j=1}^{7}\phi_{4j}^{-1}(1)G_j(1). \quad (29)$$

With K_i determined from eqn (29) we finally obtain the solution $X_i = X_{p_i} + W_i$.

Appropriate substitution in eqn (12), and employment of the non-dimensionalization eqn (16) and of eqn (19) yield the following expressions for the non-dimensional interlaminar tangential and normal stresses:

$$T_1=\left(\frac{\varphi^2 f_1}{2}+\frac{\varphi^2 f_2 A_3}{2A_9}\right)X_1''-\left(\frac{\varphi^2 f_1}{12}+\frac{\varphi f_2 A_8}{2A_9}\right)X_3'+f_3X_2$$
$$+\left(\frac{\varphi f_2}{2}+\frac{\varphi f_2 A_{10}}{2A_9}\right)X_5-\left(\frac{\varphi}{2}-\frac{\varphi f_2}{2A_9}\right)\beta m'$$

$$T_2=-\left(\frac{\varphi^2 f_1}{2}+\frac{\varphi^2 f_2 A_3}{2A_9}\right)X_1''-\left(\frac{\varphi^2 f_1}{12}-\frac{\varphi f_2 A_8}{2A_9}\right)X_3'+f_3X_2$$
$$-\left(\frac{\varphi f_2}{2}+\frac{\varphi f_2 A_{10}}{2A_9}\right)X_5+\left(\frac{\varphi}{2}-\frac{\varphi f_2}{2A_9}\right)\beta m'$$

$$P=\left(\varphi f_2+\frac{\varphi f_1 A_3}{A_9}\right)X_1'-\frac{f_1A_8}{A_9}X_3+\left(f_1+\frac{f_1A_{10}}{A_9}\right)X_4-\left(1-\frac{f_1}{A_9}\right)\beta m. \quad (30)$$

In (30), $(T_1, T_2, P) = (q_1, q_2, p_1)\,(3\Lambda_c+2\mu_c)$.

E. *Solution of a double strap joint*

As for a double strap joint shown in Fig. 1b, we have to consider two parts of adhesive and adherent, $x < \varphi$ and $x \geqslant \varphi$, separately. At the left part ($\varphi \geqslant x \geqslant 0$) the filler is the same as the adhesive layer. Then $f_4 = f_1, f_5 = f_2, f_6 = 1$, we may obtain the field equations as

$$[A]_L\{x'\}_L=[B]_L\{x\}_L+\{C\}_L. \quad (31)$$

The right part ($1 \geqslant x \geqslant \varphi$) is the central adherent of half overlap length. Similarly, we obtain

$$[A]_r\{x'\}_r=[B]_r\{x\}_r+\{C\}_r. \quad (32)$$

The boundary conditions at $x = 0$ are

$$x_{1L}(0)=0,\quad x_{2L}(0)=0,\quad x_{5L}(0)=0,\quad 4\eta x_{7L}(0)-3x_{3L}'(0)-6x_{1L}''(0)=0. \quad (33)$$

At $x = l$ they are

$$4\eta x_{7r}(l) - 3x'_{3r}(l) - 6x''_{1r}(l) = 0$$

$$4\eta x_{6r}(l) - 3x_{3r}(l) - 6x'_{1r}(l) = 0$$

$$R_{1r}x'_{1r}(l) + R_{2r}x_{3r}(l) - R_{3r}x_{6r}(l) + R_{4r}x_{4r}(l) + R_{5r}m(l) = 0. \tag{34}$$

At the interface $x = \varphi$ they are

$$x_{1L}(\varphi) = x_{1r}(\varphi), \quad x_{2L}(\varphi) = x_{2r}(\varphi) \quad x_{4L}(\varphi) = x_{4r}(\varphi), \quad x_{5L}(\varphi) = x_{5r}(\varphi)$$

$$4\eta x_{7L}(\varphi) - 3x'_{3L}(\varphi) - 6x''_{1L}(\varphi) = 4\eta x_{7r}(\varphi) - 3x'_{3r}(\varphi) - 6x''_{1r}(\varphi)$$

$$4\eta x_{6L}(\varphi) - 3x'_{3L}(\varphi) - 6x''_{1L}(\varphi) = 4\eta x_{6r}(\varphi) - 3x'_{3r}(\varphi) - 6x''_{1r}(\varphi)$$

$$R_{1L}x'_{1L}(\varphi) + R_{2L}x'_{3L}(\varphi) + R_{3L}x_{6L}(\varphi) + R_{4L}x_{4L}(\varphi) + R_{5L}m(\varphi)$$

$$= R_{1r}x'_{1r}(\varphi) + R_{2r}x'_{3r}(\varphi) + R_{3r}x_{6r}(\varphi) + R_{4r}x_{4r}(\varphi) + R_{5r}m(\varphi). \tag{35}$$

Hence, we finally obtain a system of 14 equations of 14 unknowns with a total of 14 boundary conditions, i.e. eqns (33)–(35). Substituting the unique solutions of $\{x\}_L$ and $\{x\}_r$ into eqn (30), we may obtain the interfacial stresses for both parts.

LINEAR VISCOELASTIC SOLUTION

Most engineering materials exhibit creep and relaxation behavior which depends strongly on temperature, stress level and loading duration. Certain materials, such as clay, concrete, resin, and some polymers are influenced appreciably by moisture content as well. Therefore, the need for us to have a good understanding of time-dependent behavior has accelerated in recent years. The theory of linear viscoelasticity is widely used today in characterizing polymeric materials. This theory is applicable, in principle, to all materials if the applied loads are sufficiently small. Hence, we adopt the theory to express the stress–time feature of the moisture sorption in the adhesive layer.

The basis for the stress analysis of double-lap joints bonded with a viscoelastic adhesive is the theory of linear viscoelastic stress analysis. A viscoelastic problelm is generally solved by the Alfrey (1944) correspondence principle. In the correspondence principle, Laplace transforms of the time-dependent boundary conditions and field equations are used to reduce the viscoelastic problem to an associated elastic problem. Then, elastic analysis is applied to get the associated elastic solution of the transformed equations. Inversion of the associated elastic solution results in the desired viscoelastic solution.

We now adopt the linear viscoelastic stress–strain relation (Schapery, 1980) to describe the adhesive behavior, that is

$$\sigma_{ij} = \int_0^t C_{ij}^{kl}(t-\tau)\frac{\partial \varepsilon_{kl}}{\partial \tau}\,d\tau \tag{36}$$

with the boundary conditions

$$u_i = U_i \quad \text{on} \quad S_u$$

$$\sigma_{ij}n_j = T_i \quad \text{on} \quad S_T \tag{37}$$

where U_i and T_i represent displacement and traction at i, and S_u and S_T denote surface displacement and force.

By Laplace transformation of eqns (36) and (37) we obtain

$$\bar{\sigma}_{ij} = s\bar{C}_{ij}^{kl}\bar{\varepsilon}_{kl}$$

$$\bar{u}_i = \bar{U}_i \quad \text{on} \quad S_u$$

$$\bar{\sigma}_{ij}n_j = \bar{T}_i \quad \text{on} \quad S_T \tag{38}$$

where s is the variable of its Laplace transform. S_u and S_T do not necessarily change with time.

Schapery (1967) derived the stress–strain relationship with the moisture expansion coefficient independent of time, that is

$$\sigma_{ij} = \int_0^t C_{ij}^{kl}(t-\tau)\frac{\partial \varepsilon_{kl}}{\partial \tau}\,d\tau - \beta_{ij}(t)V \tag{39}$$

where $V = C_{ij}^{kl}(t)m$.

Assuming the adhesive is homogeneous and isotropic, we can write

$$\begin{aligned} \beta_{ij} &= \beta \\ C_{ij}^{kl}(t) &= C_{ij}^{*kl}E(t) \end{aligned} \tag{40}$$

where C_{ij}^{*kl} is a constant and $E(t)$ is the tension modulus. Then eqn (39) can be reduced to

$$\sigma_{ij} = \int_0^t C_{ij}^{*kl}E(t-\tau)\frac{\partial \varepsilon_{kl}}{\partial \tau}\,d\tau - \beta V. \tag{41}$$

By Laplace transformation of eqn (41), we obtain

$$\bar{\sigma}_{ij} = sC_{ij}^{*kl}\bar{E}\bar{\varepsilon}_{kl} - \frac{\beta}{s}V. \tag{42}$$

For simplicity, replacing all the material constants and moisture expansion coefficient in the elastic solution correspondingly by the form of sC_{ij}^{*kl} and β/s as expressed in eqn (42), then we receive the viscoelastic solution in the domain of Laplace transform. In order to solve it reversely we adopt Schapery's Direct Method (Schapery, 1967); if $\sigma(t)$ has a small curvature when plotted against the logarithm of time, then

$$\sigma_{VE}(t) \approx s\bar{\sigma}_{VE}(s)_{s=1/2t} \tag{43}$$

for all positive values of s, where s is the variable of its Laplace transform.

For many adhesives, Weitsman (1980) suggested that the creep under constant stress can be expressed by a power law compliance:

$$D(t) = D_0 + D_1 t^g \tag{44}$$

where D_0 is the instantaneous compliance, and D_1 and g are material parameters. We note, however, that the elastic stresses in eqn (41) are expressed in terms of moduli. Therefore, we shall employ the highly accurate, though approximate, inversion formula which relates the relaxation modulus $E(t)$ to the creep compliance $D(t)$, in Laplace transform

$$\bar{D} = \frac{D_0}{s} + D_1\frac{\Gamma(1+g)}{s^{1+g}}. \tag{45}$$

Since

$$\bar{E}\bar{D} = \frac{1}{s^2} \tag{46}$$

then

$$\bar{E} = \frac{1}{s^2\bar{D}} = \left[s^2\left(\frac{D_0}{s} + D_1\frac{\Gamma(1+g)}{s^{1+g}}\right)\right]^{-1}. \tag{47}$$

For typical values of epoxy adhesives we choose $D_0 = 2 \times 10^{-6}$ (psi)$^{-1}$, $D_1 = 0.2 \times 10^{-6}$, $g = 0.2$ and $\beta = 0.03$ to compute the approximate viscoelastic solution.

THE FINITE ELEMENT METHOD

In comparison with linear elastic and viscoelastic solutions, one-quarter of the double-lap joint is analyzed because of symmetry about the x and z axes by the finite element method to yield a good approximation. Herein, we adopt the second order element for time and space savings with eight nodes, having worked out the third order element and found that their results were very close. Obviously, we know that the critical sections of the joint are at or near the edges of the overlap where the magnitudes of the stresses and their gradients are high. Therefore, the joint is divided into a mesh of elements of different sizes, i.e., small elements in regions where the stress gradients are high, and large elements in regions where the stresses are almost uniform.

In this work we consider it as a one-axis problem, the x-axis. The FEM meshes are shown in Fig. 2 for the first quadrant of the joint, which includes 484 elements and 1583 nodes. The line segments in the x–z plane are chosen such that the finite element mesh is finer in the areas of high stress gradients. The computer program SAP 6 is used for this task. The maximum aspect ratio of an element is 10 and occurs in the middle two-thirds of the overlap. The minimum aspect ratio of one occurs in the area of high stress gradients. The differences in the geometries of the various joints analyzed are incorporated with as little change in the finite element mesh as possible.

NUMERICAL RESULTS

In our computations we considered $h = 1.27$ cm (0.5"), $a = 0.254$ cm (0.1") and $c = 2.54$ cm (1"). The material properties were selected to represent an epoxy adhesive and aluminum adherents; hence $E_e = 3.45 \times 10^6$ kPa (5×10^5 psi), $\nu_e = 0.35$, $E = 6.895 \times 10^7$ kPa (10^7 psi), and $\nu = 0.3$. Although the adhesive layer thickness is thin in practice, we chose a very thick adhesive to avoid very large aspect ratios of the element and to save computing time. The moisture expansion coefficient was taken as $\beta = 0.03$. This coefficient relates linear strain due to moisture weight gain at 100% relative humidity.

Calculations were performed for $m(x) = m_1 + (1 - m_1)x^2$, for $m(x) = 1 - (1 - m_2)x^2$, and for $m(x) = 1$. The first of those cases, with $m_1 = 0.25$, represents the state of moisture

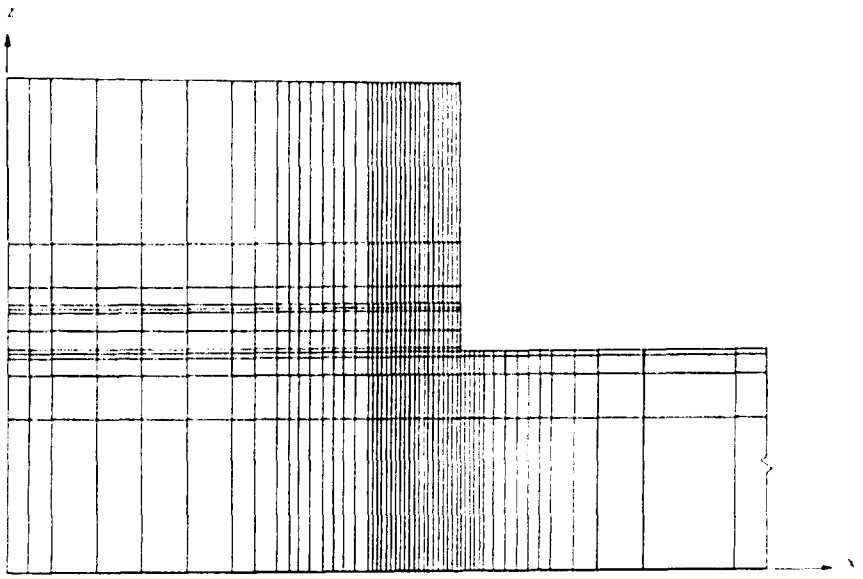

Fig. 2. The FEM meshes of the first quadrant.

absorption from the exposed locations $x = 1$, e.g., the free edge of the first quadrant non-dimensional distance from the origin. The second case, with $m_2 = 0.25$, demonstrates the stage of moisture desorption, while $m(x) = 1$ signifies equilibrium moisture content. Although none of the above non-uniform distributions corresponds to a solution of the diffusion equation, these parabolic moisture profiles enable an analytic evaluation of the linear elastic solution, thus substantially reducing the numerical effort while still demonstrating the basic features of our problem.

The results are shown in Figs 3–14, where non-dimensional values of stresses versus distance are given. To obtain dimensional values we must multiply displacements by a and stresses by $(3\Lambda_c + 2\mu_c)$. Figure 3 shows the non-dimensional displacement w_2 of the overlapping adherents vs the non-dimensional coordinate x, while Fig. 4 illustrates the non-dimensional peeling stress P vs x. In this figure and the figures for stresses hereafter, "ELASTIC" denotes the linear elastic numerical result calculated from eqn (30) for a symmetric, double lap joint, "FILLER" means the linear elastic numerical result calculated by FEM instead of the Section E solution of a double strap joint without tedious computation, while "V.E." represents the linear viscoelastic solution for a symmetric, double lap joint at the time change, and "F.E.M." illustrates the numerical FEM result by SAP 6 for a symmetric, double lap joint. Figures 5 and 6 express the interlaminar shear stresses T_1

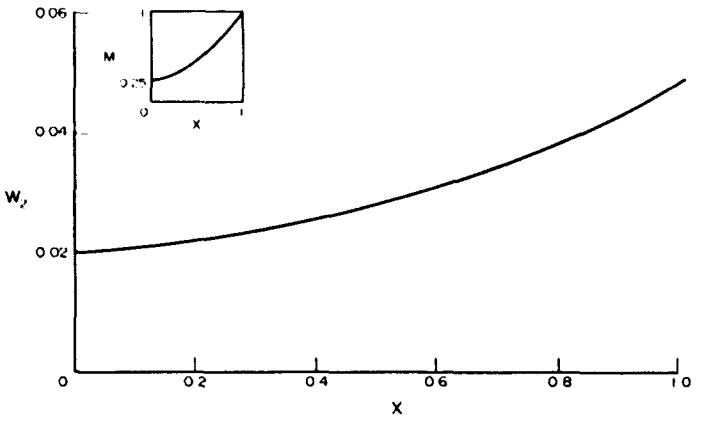

Fig. 3. The non-dimensional displacement W_2 of the outer adherents vs the non-dimensional distance x for the first case of moisture absorption.

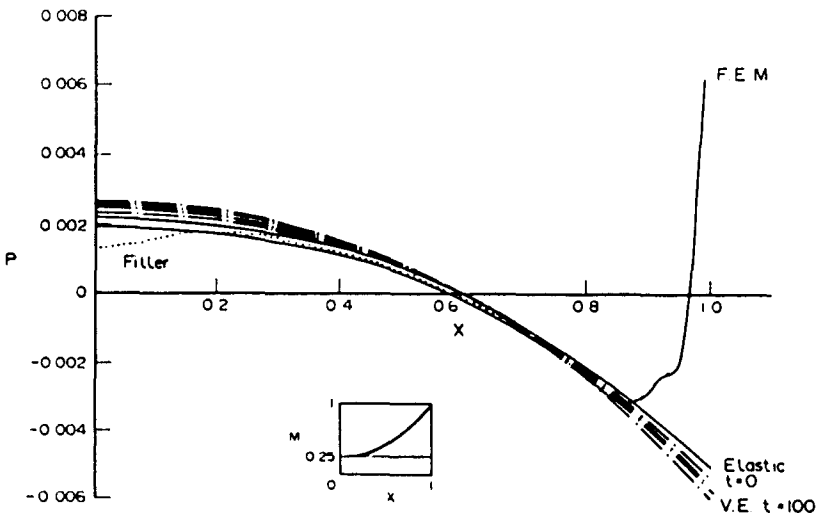

Fig. 4. The non-dimensional peel stress P vs the non-dimensional distance x for the first case of moisture absorption.

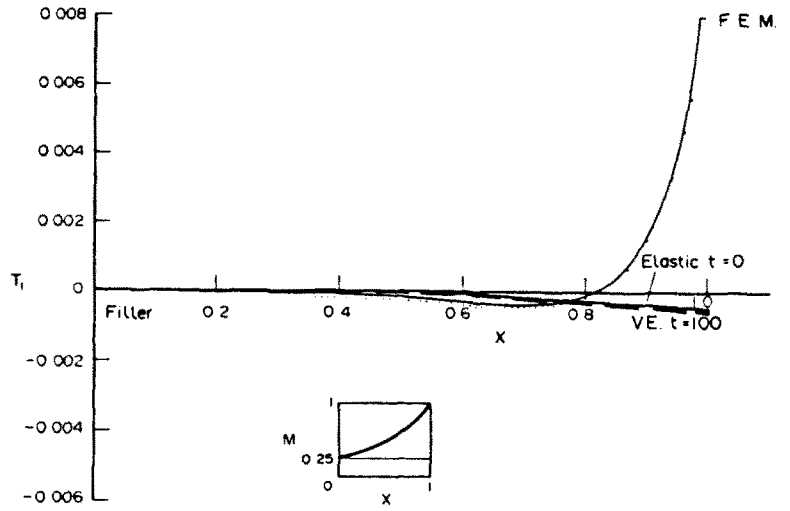

Fig. 5. The non-dimensional interlaminar shear stress T_1 vs the non-dimensional distance x for the first case of moisture absorption.

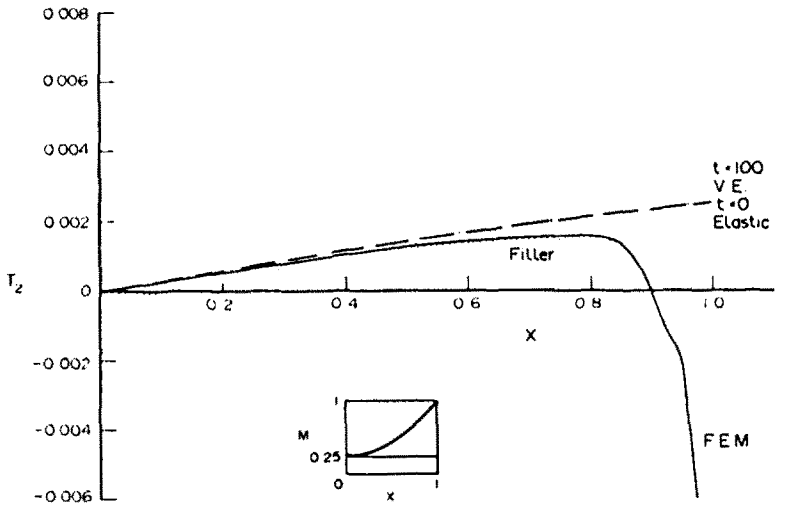

Fig. 6. The non-dimensional interlaminar shear stress T_2 vs the non-dimensional distance x for the first case of moisture absorption.

and T_2 vs x. Figures 3–6 correspond to the first case of moisture absorption, as shown in the insert. The moisture sorption modeled in SAP 6 can be taken for granted as the temperature effect shown in the User Manual.

The normal stress P and interlaminar shear stresses T_1 and T_2 of FEM curves are the data taken from the interfaces. Near the free edge these stresses behave singularly with a big jump of the highest absolute value. Figures 7–10 and 11–14 are analogous to Figs 3–6, but are unrelated to the second case of moisture desorption and to a uniform equilibrium moisture distribution, respectively. In each case the moisture distribution is shown in the insert.

DISCUSSIONS

Note the opposite trends exhibited by the results of Figs 3–6 on one hand and Figs 7–10 on the other for elastic and viscoelastic solutions. During moisture absorption the outer adherents possess positive curvatures and the maximal peel stresses are compressive. This

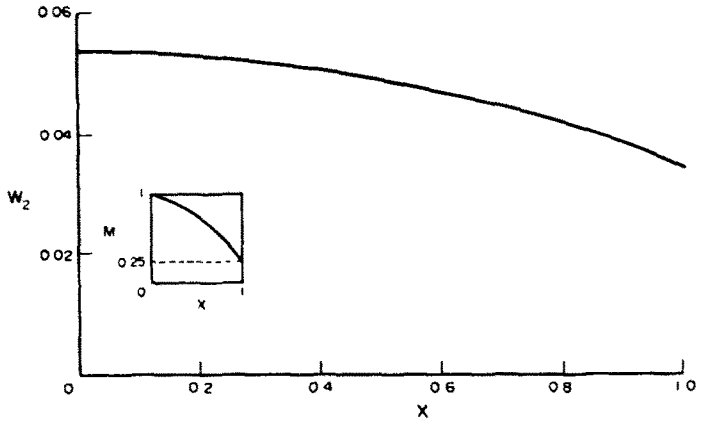

Fig. 7. The non-dimensional displacement W'_2 of the outer adherents vs the non-dimensional distance x for the second case of moisture absorption.

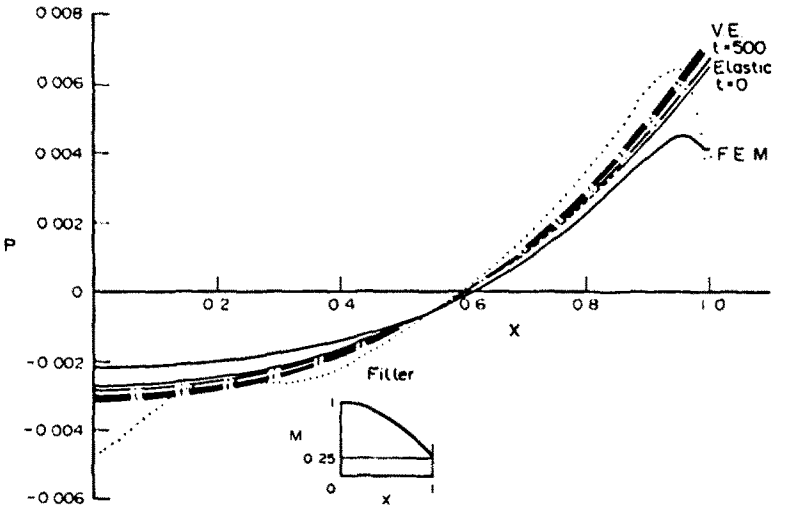

Fig. 8. The non-dimensional peel stress P vs the non-dimensional distance x for the second case of moisture desorption.

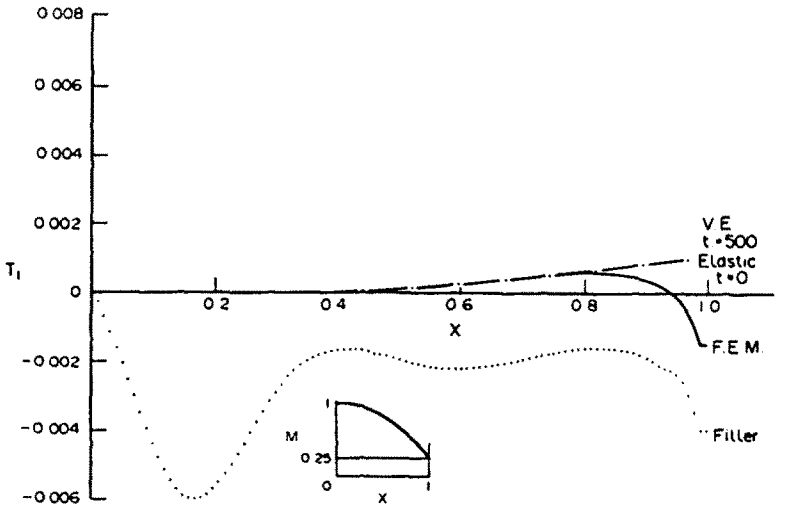

Fig. 9. The non-dimensional interlaminar shear stress T_1 vs the non-dimensional distance x for the second case of moisture desorption.

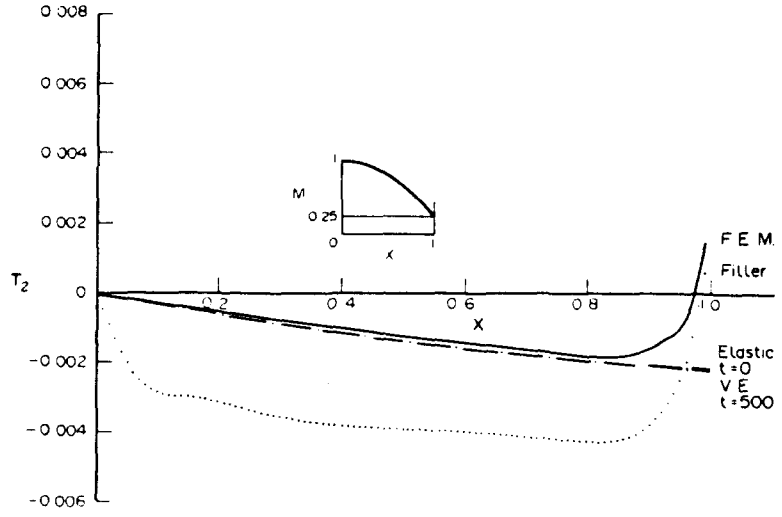

Fig. 10. The non-dimensional interlaminar shear stress T_2 vs the non-dimensional distance x for the second case of moisture desorption.

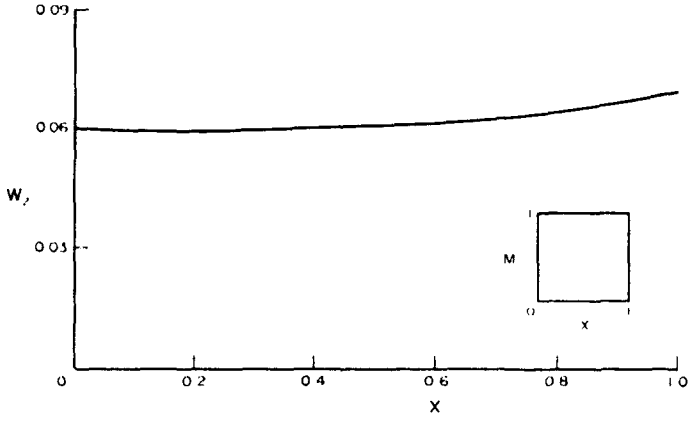

Fig. 11. The non-dimensional displacement W_2 of the outer adherents vs the non-dimensional distance x for a uniform equilibrium moisture distribution.

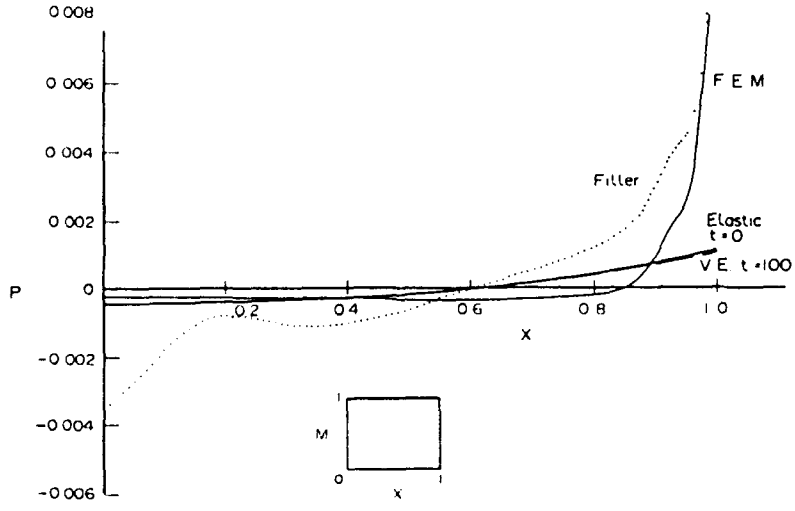

Fig. 12. The non-dimensional peel stress P vs the non-dimensional distance x for a uniform equilibrium moisture distribution.

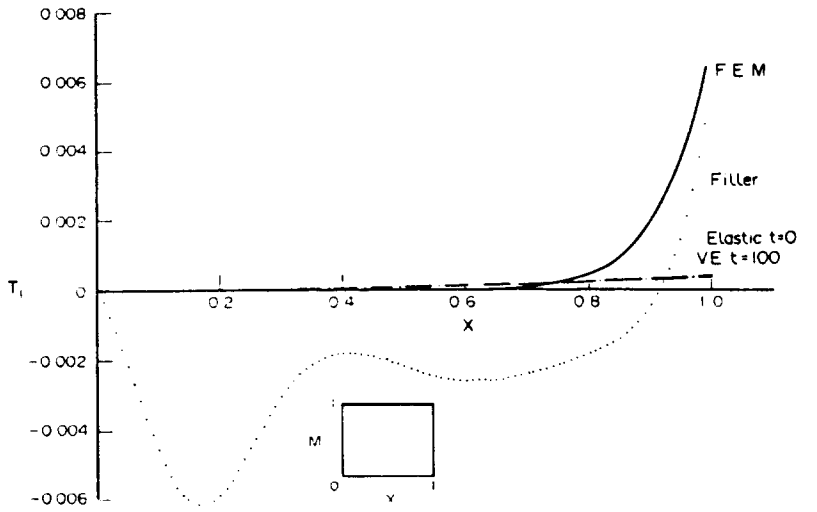

Fig. 13. The non-dimensional interlaminar stress T_1 vs the non-dimensional distance x for a uniform equilibrium moisture distribution.

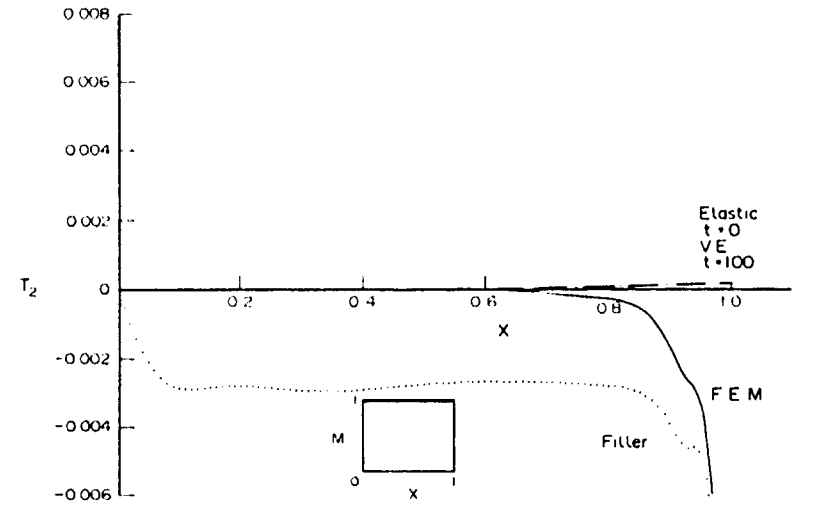

Fig. 14. The non-dimensional interlaminar stress T_2 vs the non-dimensional distance x for a uniform equilibrium moisture distribution.

situation reverses itself upon desorption, which is accompanied by severe tensile stresses. The observation leads us to conclude that desorption is generally more detrimental to the integrity of the joint. We also note a reversal in the signs of the interlaminar shear stresses, when comparing the absorption and desorption cases. Furthermore, in both cases T_1 and T_2 are of opposite sign, a fact which points to the severity of the shear effects within the adhesive layer, especially near the free edge where a theoretical singularity is predicted by elasticity theory. The case of uniform equilibrium moisture distribution, shown in Figs 11 - 14, indicates that although the outer adherents displace with only slight bending, the joint nevertheless sustains substantial stresses. These stresses are attributable to the discrepancy between the moduli of the adhesive and adherent materials.

The absolute value of the viscoelastic solution becomes slightly larger than that of the elastic solution as the time increases for peeling stress in both absorption and desorption cases due to the decrease of relaxation modulus $E(t)$, i.e., the adhesive becomes softer. The stiffness difference between decreasing $E(t)$ of adhesive and unchanged adherent will become more significant with increasing time, which results in the slightly larger viscoelastic stresses. As for interlaminar shear stresses both solutions have no difference. The curves of both

cases almost intersect at $x = 0.6$. Similarly, for the equilibrium case both solutions are very close even for very long time, because weight gain of moisture will not increase, i.e. it is independent of time. In comparison with the thermal expansion coefficient we find that the moisture content change is a very very slow process and its influence is a long-term effect. Hence, we may neglect the moisture effect for a very short time.

As predicted by elasticity the theoretical singularity at the free edge is verified by the FEM. The FEM results are very close to the elastic solution at $0 \leqslant x \leqslant 0.6$ and deviated slightly at $0.6 < x \leqslant 0.8$. While at $x > 0.8$ the stresses increase toward the free edge, we have made even more refinements near the free edge. In most situations the singular stresses of peel and shear are opposite to the elastic values at the free edge due to random divergence of the computer program used to treat the singular problem. This problem is similar to free edges of composite laminates; we can solve it by finding the order of singularity first and compute interlaminar stresses (Jen *et al.*, 1990a,b).

For a double strap joint, shown in Fig. 1b, the tiny gap between the central adherents is filled with adhesive which is the same material as the adhesive layer. We have also obtained the values of stresses denoted by "FILLER" in the figures. In the first case of absorption the stresses are close to the result of FEM at $0 \leqslant x < 0.2$. In the desorption and equilibrium cases the filler has a large influence on the stresses of peel and shear and the change is not limited to a small part near the gap. Berg (1970) analyzed a bonded double lap joint and suggested interleaving the materials of a gap joint to reduce the high stresses that otherwise occur where the layers meet. Hence, the symmetric, double lap joint is better than the double strap due to the environmental effect of resisting smaller residual stresses.

CONCLUSIONS

This paper presented solutions to sample problems which demonstrate the effects of non-uniform moisture profiles on the residual stress field in bonded joints.

First, the solutions are derived for a linearly elastic response of both adhesive and adherent materials which are based upon restrictively kinematical assumptions. We then extend them to apply to the linear viscoelastic response, and verify them by using the FEM to be suitable for double strap joints. Parametric studies, which involved the computation of interlaminar stresses for increasingly stiffer adherents, indicated that the peel stresses tended to increase and the magnitudes of the shear stresses remained substantially unchanged. The last observation indicates that the kinematical assumptions employed in this paper restrict the validity of our results to adhesive bond lines which are not excessively thin and our conclusions can serve as guidelines only under these limitations. A comprehensive treatment of the problem presented herein involves the incorporation of the inelastic and non-linear constitutive behavior of the adhesive. Such treatment should be based on numerical formulations and solutions. Finally, we suggest that in the consideration of environmental effects on adhesives, the interaction of both moisture and temperature should be paid attention to in further research.

Acknowledgements—The authors wish to thank Profs Y. Weitsman and P. W. Bates at Texas A&M University for many helpful instructions and suggestions.

REFERENCES

Alfrey, T. (1944). Non-homogeneous stresses in visco-elastic media. *Quart. Appl. Math.* **2**, 113–119.
Berg, K. R. (1970). Problelm in the design of joints and attachments. In *Mechanics of Composite Materials. Proc. 5th Symp. Naval Structural Mechanics* (Edited by F. W. Wendt, H. Liebowitz and I. V. Perrone), pp. 467–479. Pergamon Press, New York.
Coddington, E. A. and Levinson, N. (1955). *Theory of Ordinary Differential Equations*. McGraw-Hill, New York.
Crossman, F. W., *et al.* (1979). Hydrothermal damage mechanisms in graphite/epoxy composites. NASA 2-0563, Lockheed Palo Alto Research Lab.
Donnell, L. H. (1976). *Beams, Plates and Shells*. McGraw-Hill, New York.
Dym, C. L. and Shames, I. H. (1973). *Solid Mechanics: A Variational Approach*. McGraw-Hill, New York.
Flaggs, D. L. and Crossman, F. W. (1979). *Viscoelastic Response of a Bonded Joint due to Transient Hydrothermal Exposure* (Edited by J. R. Vinson), pp. 299–314. ASME, New York.
Hochstadt, H. (1963). *Differential Equations: A Modern Approach*. Holt, Rinehart & Winston.

Hoskin, B. C. and Baker, A. A. (1986). *Composite Materials for Aircraft structures*, AIAA Education Series. AIAA, New York.
Jen, M.-H. R. (1980). Stresses in adhesive joints due to moisture sorption. M.Sc. Thesis, Texas A&M University.
Jen, M.-H. R. and Weitsman, Y. (1981). Stresses in adhesive joints due to moisture sorption. ASME Publication AD-1, pp. 67–74.
Jen M.-H. R., Hsu, J. M. and Kau, Y. S. (1990a). Interlaminar stresses in a centrally notched cross-ply composite laminate. *J. Appl. Mech.* (submitted).
Jen, M.-H. R., Hsu, J. M., Kau, Y. S. and Kao, P. W. (1990b). The interlaminar stresses at straight edges in composite laminates. *Int. J. Reinforced Plastics Compos.* (in press).
Kolman, B. (1965). *Elementary Linear Algebra*. Macmillan, New York.
Ramanko, J. and Kanus, W. G. (1980). Fatigue behavior of adhesively bonded joints. AFWL-TR-80, General Dynamic Corp., Fort Worth Division.
SAP 6 (1982). *A Structural Analysis Program for Static and Dynamic Analysis*, User's Manual, SAP Users Group, University of Southern California.
Schapery, R. A. (1967). Stress analysis of viscoelastic composite materials. *J. Compos. Mater.* **1**, 228.
Schapery, R. A. (1980). Class Notes, Materials and Mechanics Center, Civil Engineering Department, Texas A&M University, College Station, TX.
Schwartz, M. M. (1984). *Composite Materials Handbook*. McGraw-Hill, New York.
Schwartz, S. S. and Goodman, S. H. (1982). *Plastics Materials and Process*. McGraw-Hill, New York.
Weitsman, Y. (1977a). Stresses in adhesive joints due to moisture and temperature. *J. Compos. Mater.* **6**, 378–394.
Weitsman, Y. (1977b). Effects of fluctuating moisture and temperature on the mechanical response of resin-plates. *J. Appl. Mech., ASME* **44**, 571–576.
Weitsman, Y. (1979). Interfacial stresses in viscoelastic adhesive layers due to moisture sorption. *Int. J. Solids Structures* **15**, 701–714.
Weitsman, Y. (1980). Residual thermal stresses in a symmetric double-lap joint. *J. Thermal Stresses* **3**, 521–535.

APPENDIX

The following expressions define the constants employed in this paper:

$$A_1 = f_4\eta + f_1\varphi + f_6\eta, \quad A_2 = \tfrac{1}{2}\eta(f_6 - f_4), \quad A_3 = f_5 - f_2, \quad A_4 = -\tfrac{1}{2}f_6\eta^2, \quad A_5 = f_2,$$

$$A_6 = -\tfrac{1}{4}(f_4 + f_6)\eta\varphi - \tfrac{1}{12}f_1\varphi^2, \quad A_7 = f_3, \quad A_8 = \tfrac{1}{2}f_5\varphi, \quad A_9 = f\frac{\varphi}{4\eta} + f_3, \quad A_{10} = -f_3. \tag{A1}$$

$$B_1 = A_1 - \frac{\varphi A_7^2}{A_9}, \quad B_2 = A_2 + \frac{A_8 A_7}{A_9}, \quad B_3 = A_4, \quad B_4 = A_5 - \frac{A_{10}A_7}{A_9}, \quad B_7 = A_7,$$

$$B_{11} = \varphi B_4, \quad B_{13} = -A_{10}\left(1 + \frac{A_{10}}{A_9}\right), \quad B_{14} = k_2 A_7 + \frac{A_8 A_{10}}{A_9}, \quad B_{15} = (k_1 - \tfrac{1}{2}\varphi k_2 - \tfrac{3}{8}\varphi\eta)A_4,$$

$$B_{16} = k_1 B_4 - k_2\frac{A_8 A_{10}}{A_9}, \quad B_{17} = A_6 + \frac{A_8^2}{A_9} + \varphi\frac{B_2^2}{B_1}, \quad B_{18} = -\varphi\frac{A_4}{2} + \varphi\frac{B_1 B_2}{B_1}, \quad B_{19} = \varphi\frac{B_4 B_2}{B_1} - \frac{A_8 A_{10}}{A_9},$$

$$B_{20} = B_1\left(A_6 + \frac{A_8^2}{A_9}\right) + \varphi B_2^2, \quad B_{21} = \varphi A_4\left(A_6 + \frac{A_8^2}{A_9} + \varphi\frac{B_2}{2}\right), \quad B_{22} = \varphi A_4\left(B_2 - \frac{B_1}{2}\right), \quad C_1 = 1 + \frac{A_7}{A_9},$$

$$C_3 = 1 + \frac{A_{10}}{A_9}, \quad C_4 = k_1 C_1 + k_2\frac{A_8}{A_9}, \quad C_5 = \frac{\varphi B_2}{B_1}C_1 + \frac{A_8}{A_9}$$

where

$$k_1 = -\frac{B_{21}}{B_{20}}, \quad k_2 = \frac{B_{22}}{B_{20}}. \tag{A2}$$

$$R_1 = F_6 - f_4 - \frac{f_5(f_2 - f_5)\varphi}{f_4\varphi + f_1\eta}, \quad R_2 = \tfrac{1}{2}(f_6 - f_4) + \tfrac{1}{6}f_1\varphi\eta - \frac{f\frac{3}{8}\varphi}{2(f_4\varphi + f_1\eta)},$$

$$R_3 = -\tfrac{1}{2}f_6\eta, \quad R_4 = -\frac{f f_5}{f_4\varphi + f_1}, \quad R_5 = -\frac{f_5}{f_4\varphi + f_1\eta}. \tag{A3}$$

$$k_{13} = -\frac{B_2 B_{11} B_{13}}{d}, \quad k_{14} = -\frac{B_4 B_{11} B_{13}}{d}, \quad k_{16} = -\frac{B_3 B_{11} B_{13}}{d}, \quad k_{12} = -\frac{B_1 B_6 B_{11}}{d},$$

$$k_{15} = -\frac{B_1 B_{11} B_{15}}{d}, \quad k_{17} = -\frac{B_2 B_{11} B_{14}}{d}, \quad k_{73} = \frac{B_{13}(-B_2 B_4 - B_1 B_{16})}{d}, \quad k_{74} = \frac{B_{13}(-B_4^2 - B_1 B_9)}{d},$$

$$k_{76} = \frac{B_{13}(-B_1 B_4 - B_1 B_2)}{d}, \quad \text{and} \quad d = \det[D]. \tag{A4}$$